Coastal Engineering 73 (2013) 71–83

Contents lists available at SciVerse ScienceDirect

Coastal Engineering

journal homepage: www.elsevier.com/locate/coastaleng

Wave damping over artificial *Posidonia oceanica* meadow: A large-scale experimental study

Theoharris Koftis [a,*], Panayotis Prinos [a], Vasiliki Stratigaki [b]

[a] Hydraulics Laboratory, Department of Civil Engineering, Aristotle University of Thessaloniki, Thessaloniki, 54124, Greece
[b] Department of Civil Engineering, Ghent University, Technologiepark 904, Zwijnaarde, B-9052, Belgium

ARTICLE INFO

Article history:
Received 15 September 2011
Received in revised form 18 October 2012
Accepted 24 October 2012
Available online 16 November 2012

Keywords:
Posidonia oceanica
Wave damping
Drag coefficient
Velocity attenuation
Artificial sea grass
Large scale experiment

ABSTRACT

An experimental study, conducted in the large wave flume of CIEM in Barcelona, is presented to evaluate the effects of *Posidonia oceanica* meadows on the wave height damping and on the wave induced velocities. The experiments were performed for irregular waves from intermediate to shallow waters with the dispersion parameter h/λ ranging from 0.09 to 0.29. Various configurations of the artificial *P. oceanica* meadow were tested for two stem density patterns (360 and 180 stems/m^2) and for plant's height ranging from 1/3 to 1/2 of the water depth.

The results for wave height attenuation are in good agreement with the analytical expressions found in literature, based on the assumption that the energy loss over the vegetated field is due to the drag forces. Based on this hypothesis, an empirical relationship for the drag coefficient related to the Reynolds number, Re, is proposed. The Reynolds number, calculated using the artificial *P. oceanica* leaf width as the length scale and the maximum orbital velocity over the meadow edge as the characteristic velocity scale, ranges from 1000 to 3500 and the drag coefficient C_d ranges from 0.75 to 2.0.

The calculated wave heights, using the analytical expression from literature and the proposed relationship for the estimation of C_d, are in satisfactory agreement with those measured. Wave orbital velocities are shown to be significantly attenuated inside the meadow and just above the flume bed as indicated by the calculation of an attenuation parameter. Near the meadow edge, energy transfer is found in spectral wave velocities from the longer to the shorter wave period components. From the analysis it is shown that the submerged vegetation attenuates mostly longer waves.

1. Introduction

Sustainable protection of coastal areas with respect to the marine ecosystem is of high importance and bioengineering can be a novel tool for such service. Bioengineering is the use of living materials such as plants or reef builders to alleviate the need of hard construction measures (de Oude et al., 2010). This need for mitigation of wave action and/or flooding and coastal erosion hazards with low environmental impact on the coastal environment can be satisfied with the use of natural coastal defense "structures" such as seagrass meadows.

Seagrasses are marine plants that have roots, stems and leaves. From approximately 50 species worldwide (den Hartog, 1977) *Posidonia oceanica* is the most common seagrass species in the Mediterranean Sea and is usually distributed from shallow subtidal waters to a depth of 50 m in clear conditions (Borum et al., 2004). *P. oceanica* can colonize soft substrates such as sand in wave-sheltered areas and also attach to rocks being exposed to relatively high wave energy and wind driven currents (Koch et al., 2006). The importance of seagrasses regarding biological and physical aspects has been well recognized; due to their capacity to alter their environment, seagrasses have been referred to as "ecosystem engineers". Seagrass meadows are of great importance for maintaining biodiversity since they are highly productive and can serve as important nursery grounds for numerous species of algae, fish and invertebrates both above and below the seabed (Green and Short, 2003). Regarding the coastal protection aspect, a service commonly listed for seagrasses is sediment and shoreline stabilization, achieved by slowing down water motion and current flow and by reducing sediment suspension (Borum et al., 2004; Fonseca and Cahalan, 1992). In the Tigny et al. (2007) field study, the same effects are found; *P. oceanica* meadows significantly affect the littoral geomorphology, providing biogenic sediments, controlling beach slope, and acting as a "brake" on coastal water masses.

With regard to the wave and seagrass interaction, a complex water flow system describes the situation, since not only water flow affects seagrasses and seagrasses affect water flow but seagrasses and water flow may interact in highly coupled, nonlinear ways

* Corresponding author. Tel.: +30 2310 995877; fax: +30 2310 995672.
E-mail address: thkoftis@civil.auth.gr (T. Koftis).

0378-3839/$ – see front matter © 2012 Elsevier B.V. All rights reserved.
http://dx.doi.org/10.1016/j.coastaleng.2012.10.007

(Koch et al., 2006). The degree of wave attenuation depends both on the seagrasses' characteristics (the plant's density, the seagrass height, the stiffness of the plant and the bending of the shoots) and the wave parameters (wave height, period and direction) so the quantification of wave energy dissipation over seagrasses is difficult to express in a universal way (Mendez and Losada, 2004).

Various laboratory and field studies on wave attenuation due to seagrasses have been performed, with large variability of the results for wave damping over seagrass meadows that confirm the complexity of such flow system. Wave height reduction over vegetated seabed was studied by Fonseca and Cahalan (1992). Four common North American seagrass species; *Halodule wrihtii*, *Syringondium filiforme*, *Thalassia testudinum* and *Zostera marina* were harvested from several sites along the Florida Keys and were placed in a 6 m long wave flume. Wave height attenuation was found between 20% and 76% (~40% on average) over 1 m length when the plants were occupying the entire water depth. Artificial plants were used in the experiments of Ota et al. (2004) in a 30 m long wave flume. Each stem was formed by four leaves made of polyester and all stems constituted a 6 m long vegetated seabed with stem density of 1000 stems/m^2, occupying half the water depth. The experimental results were compared with a simple numerical model based on the linear wave theory and satisfactory agreement was found for values of the drag coefficient $C_d = 1.3$. Bradley and Houser (2009) performed a field study in a microtidal bay in northwest Florida, where the main species of the meadows were *T. testudinum* and *H. wrightii*. The study was performed for small Reynolds numbers ($200 < Re < 800$) and for these conditions they obtained large values for the drag coefficient ($1.5 < C_d < 100$) and suggested a relationship for the drag coefficient with either the Reynolds or the Keulegan–Carpenter number. The measured wave height decay for submerged vegetation was found to be described well with an exponential function proposed by Kobayashi et al. (1993) and Mendez et al. (1999). The efficient scaling and reproduction of the physical plant's flexibility by artificial meadows have been important features in most recent studies. In Elginoz et al.'s (2011) experimental study, the leaves of the artificial models were made of Nickel-chrome stripe wire with a density of $\rho = 7757$ kg/m^3 and a modulus of elasticity $E = 1.98$ GPa. The model was in a 1:10 scale compared with prototype conditions and this analogy was selected to reproduce both the wave conditions and the plant's characteristics. The model reproduced a natural meadow with 87 stems/m^2, the leaf length varied from 0.10 to 0.50 of the water depth approximately and was placed on a 1:5 slope beach at the end of the 24 m long wave flume. The results showed that the ratio of the wave height on the vegetated side to the unvegetated side is between 0.78 and 0.94. In Sánchez-González et al. (2011) the experiments were conducted also in a 1:10 geometric scale in a 46.3 m long wave flume. The artificial plant leaves were made of polyethylene and polypropylene with a density of $\rho = 900 \pm 20$ kg/m^3 and a modulus of elasticity $E = 1.6$ GPa. The results regarding wave damping were found to follow the exponential decay law and steeper waves were found to be mostly attenuated. The experiments were performed in a range of $100 < Re < 1500$ and the obtained values for the drag coefficient C_d were in the range $0.1 < C_d < 1.0$ approximately. They showed that the dependence of C_d on the Keulegan–Carpenter number, ranging from 10 to 250 approximately, is stronger than that on the Reynolds number.

The attenuation of wave induced velocities has been studied experimentally to address the ability of the plants to slow the water motion, increase sedimentation and provide efficient protection of the beaches against erosion. The interaction of flow and seagrass canopies of *Amphibolis antarctica* species, which differ morphologically from more commonly studied blade-like seagrasses such as *Zostera* and *Thalassia*, was performed in the field study of Verduin and Backhaus (2000). A series of velocity measurements were obtained within, above and adjacent to *A. antarctica* meadows for swell wave conditions of the study area ($T = 13$–16.5 s). The results showed an overall damping effect since the power spectra of the velocity data revealed a specific reduction in energy within the canopy. Granata et al. (2001) measured the particle and flow distribution within seagrass meadows in a Northeast coast of Spain for both low and high wave and current activities. The results revealed the 3-dimensionality of the meadow, showing that it acts as a bluff body diverting flow over the meadow, while producing a secondary circulation cell at the meadow's edge. Lowe et al. (2007) performed experiments with rigid cylinders representing a submerged canopy for the quantification of the wave induced velocities by the introduction of an attenuation parameter. The results showed that longer-period components in the wave spectrum are significantly more attenuated than shorter-period components. Enhancing these experimental results Lowe et al. (2008) presented a mathematical model based on porous flow to account for the wave-driven flow within the canopy. The model unknown parameters such as the friction coefficient, C_f, dimensional drag parameter, β, and inertial coefficient, C_M, were calibrated by the experimental data. Experiments with a flexible artificial canopy, made of polyethylene, with $\rho = 920$ kg/m^3 and modulus of elasticity $E = 0.3$ GPa were carried out in a 20 m long wave flume in Luhar et al. (2010). The experiments were performed for a range of parameters, stem density 300–1800 stems/m^2 and plant leaves height ranging from 1/2 to 1/1 of the water depth. The results showed that a local circulation pattern is revealed within the meadow.

Numerical modeling for such wave–seagrass interaction is a demanding task, since the parameters of the plant stiffness and movement with wave motion are difficult to model. Therefore in early theoretical and numerical studies, plants have been simulated as rigid cylinders with different values to the drag coefficient (Dalrymple et al., 1984; Kobayashi et al., 1993). Mendez and Losada (2004) developed an empirical model for wave transformation on vegetation fields that included wave damping and wave breaking over vegetation fields on variable depths. Based on a nonlinear formulation of the drag force, the model was calibrated for a specific type of plant (*Laminaria hyperborea* kelp) and the results were compared with available experimental data. Chen et al. (2007) developed a model to account for the interactions between waves, currents and sediment transport in seagrass systems within the nearshore circulation model SHORECIRC and the REF/DIF wave model. The drag coefficient C_d accounting for currents and waves was estimated based on an average drag coefficient $C_d \sim 1.17$ and accounting for the seagrass density and submergence. Li and Yan (2007) developed a three-dimensional numerical model to simulate the wave–current–vegetation interaction using the RANS equations where the extra drag force term due to vegetation takes different values depending on the nature of the flow; unidirectional flow through vegetation, wave–vegetation interaction and wave–current–vegetation interaction. The drag coefficient C_d for the wave–vegetation case was calculated using the Mendez et al., 1999 empirical expression related to the Reynolds number. Suzuki and Dijkstra (2007) used a Volume of Fluid model to simulate wave attenuation over strongly varying beds and vegetation fields, both stiff and submerged flexible artificial vegetation on a sloped bed and a flat bed. In Li and Zhang (2010) a 3D RANS model was employed for the study of the hydrodynamics and mixing induced by random waves on vegetation. The vegetation was represented as an array of cylinders with the drag coefficient expressed with the empirical expression proposed by Mendez and Losada (2004), while the results of the model were in good agreement with experimental data. Recently Huang et al. (2011) presented a numerical model based on the Boussinesq equations, for the study of the interaction of solitary waves with emergent rigid vegetation. The model used values for the drag coefficient calculated from the experimental part of the study, which were in the range of $1.41 < C_d < 2.45$.

From the above mentioned studies the following main issues regarding the wave and submerged vegetation interaction arise: (i) the degree of wave height damping (ii) the efficient numerical modeling of such flows that strongly depend on the estimation of the meadow drag coefficient and (iii) the attenuation of wave-induced velocities. The

investigation of these issues is the main objective of the present study. The large scale experiments, conducted in the CIEM wave flume at the Universitat Polytecnica de Catalunya, on irregular wave attenuation and wave flow transformations induced by artificial *P. Oceanica* meadow are analyzed. In Stratigaki et al. (2011) the results of the same CIEM experiments for regular waves over artificial *P. oceanica* meadows showed that the damping of wave height depends on seagrass density and submergence ratio. The present study enhances insight regarding the spectral wave analysis and moreover the estimation of a drag coefficient and the calculation of a velocity attenuation parameter. In particular, the study focuses on the effects of the submergence ratio $\alpha = h_s/h$ (h_s = height of seagrass, h = water depth), the seagrass density N (stems/m^2) and the wave period on the wave height attenuation. An empirical relationship for the drag coefficient C_d related to the Reynolds number, is obtained, characteristic for the *P. oceanica*, which can be useful in the numerical analysis of such wave–seagrass interactions. The effect of the above plant characteristics on the wave induced velocities is also examined. Following the analysis of Lowe et al. (2007) and Manca et al. (2010) which showed the spectral wave energy dissipation within submerged canopies is frequency-dependent, an attenuation parameter of wave induced velocities is calculated for the frequency components of the incident wave spectrum.

2. Physical model

2.1. Experimental setup

The experiments were carried out in the CIEM wave flume (Canal d'Investigació i Experimentació Marítima) at the Universitat Polytecnica de Catalunya, Barcelona. The wave flume, 100 m long, 5 m deep and 3 m wide, offers the ability to perform experiments in a prototype scale. The waves are generated by a wave paddle at the left side of the flume, and a sandy slope beach of 1:15 was formed at the opposite end, for the elimination of wave reflection. A 20 m long horizontal and flat sandy area was created in the central part of the flume and the meadow of artificial *P. oceanica* with length L = 10.70 m was placed at this horizontal part, as shown in Fig. 1.

2.2. Properties and scaling of artificial P. oceanica

The physical properties of the plant, such as the density and stiffness, are important in order to study the wave interaction, the bending of the leaves and the resulting wave damping efficiently. A typical physical *P. oceanica* stem is composed of four to eight ribbon-like leaves (Cavallaro et al., 2010; Sánchez-González et al., 2011), each of them 1 cm wide, 1 mm thick and up to 1 m long. The density of the prototype plant, ρ_S, ranges from 800 to 1200 kg/m^3 and the modulus of elasticity, E, ranges from 0.41 to 0.53 GPa as found in Folkard (2005). The plant's stem density can vary from sparse (<150 stems/m^2) found in deeper waters to dense (>700 stems/m^2).

The geometry of the artificial plant was chosen in order to reproduce that of the prototype one. Each stem of the artificial plant was composed of four leaves with 1 cm width and 1 mm thickness and variable leaf length; one pair of 35 cm long leaves, and another pair of 55 cm length. The leaves were inserted in a stiff 10.0 cm long rod, made of PVC, which was then placed in a metal board forming the artificial meadow (Fig. 2). Two different stem density patterns were reproduced; a high density configuration with N = 360 stems/m^2, representative of a dense *Posidonia* meadow patch (following Giraud, 1977 classification) and an average one, with N = 180 stems/m^2.

Regarding the mechanical properties for the model used, a dimensional analysis was performed for determining the characteristic parameters using PVC as a material for constructing the artificial *P. oceanica* meadow. The density and the modulus of elasticity of the PVC material used are 550–700 kg/m^3 and 0.903 GPa, respectively. Ghisalberti and Nepf (2002) proposed a non-dimensional parameter λ_1, for the efficient modeling of movement of the leaves; recently adopted by Sánchez-González et al. (2011). The parameter λ_1 is defined as:

$$\lambda_1 = \frac{(\rho_W - \rho_S) h_s^{\,3}}{E t^2} \tag{1}$$

where h_s and t, are the length and thickness of leaves, respectively, and ρ_w and ρ_s are the water and plant densities, respectively. Based on the above relationship, the model parameter $\lambda_{1,\,m}$ varies from 0.055 to 0.083 and is within the limits of the prototype parameter $\lambda_{1,\,p}$, since $0.001 < \lambda_{1,p} < 0.091$.

However such a relationship does not account for the effect of the flow velocity. The use of the Cauchy number, defined as the ratio of the dynamic pressure and the modulus of elasticity, which characterizes the deformation of an elastic solid under the effect of flow is more appropriate for problems of the flow–plant interaction. The Cauchy number is defined as:

$$C_y = \frac{\rho_w U^2}{E} S^3 \tag{2}$$

where U is a characteristic velocity and S is the slenderness number, defined as L/l (L = maximum cross-sectional dimension of the plant leaf and l = minimum cross-sectional dimension of the plant leaf). It should be noted that this definition includes the slenderness number S which needs to be taken into account in the deformability. It is well known that the deformation of a slender beam in bending under a transverse surface load is proportional to S^3 (Nikklas, 1992). Hence, the ratio $C_{y,m}/C_{y,p}$ (m: model and p: prototype) given in Eq. (3) shows that the artificial plant used is slightly stiffer compared to the prototype plant.

$$\frac{C_{y,m}}{C_{y,p}} = \left(\frac{U_m}{U_p}\right)^2 \left(\frac{S_m}{S_p}\right)^3 \left(\frac{E_p}{E_m}\right) = 0.45 - 0.59. \tag{3}$$

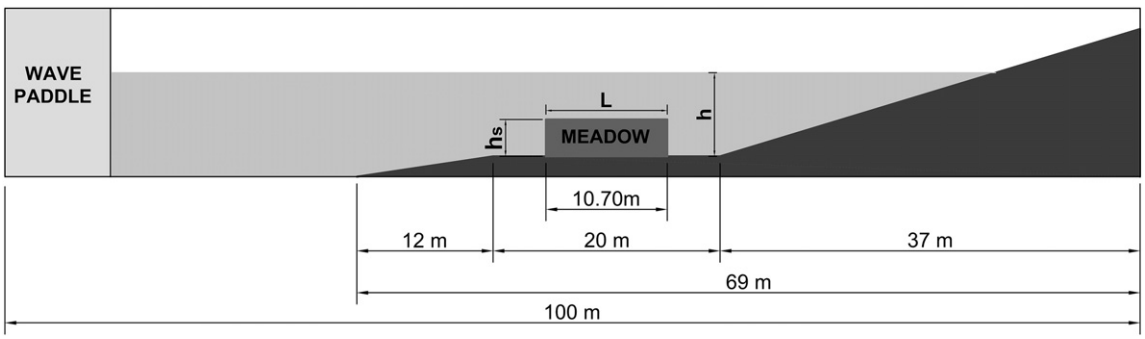

Fig. 1. Sketch of the experimental setup of the CIEM flume.

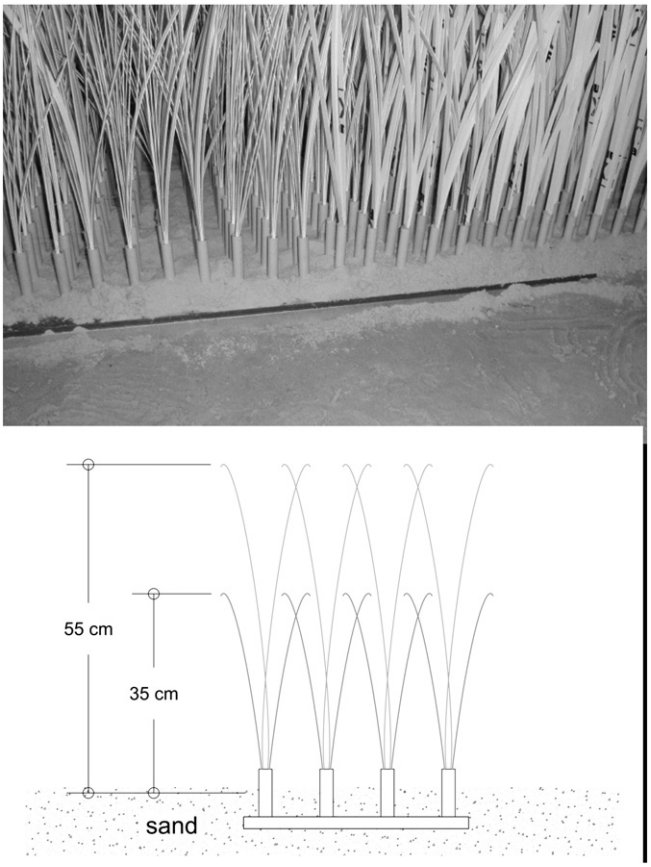

Fig. 2. Photo and schematic detail of the artificial *Posidonia oceanica* meadow.

2.3. Test conditions

A series of experiments were performed for irregular waves propagating over the artificial *P. oceanica* meadow in intermediate and shallow waters. The wave conditions were selected in order to reproduce mild wave conditions of the Mediterranean Sea where *P. oceanica* is mainly found. Jonswap spectrum, with a γ parameter equal to 3.3, was used for the generation of irregular waves with the significant wave height H_s ranging from 0.28 m to 0.40 m, the peak wave period T_p from 2.0 s to 4.5 s, thus for intermediate to shallow waters, $0.09<h/\lambda<0.29$ and for wave steepness $0.017<H/\lambda<0.052$. The water depth in the flume, at the location of the meadow, h, ranged between 1.10 m and 1.70 m, resulting in a range of the submergence ratio α ($=h_s/h$) from 0.32 to 0.50. The wave and meadow characteristics of the experiments are shown in Table 1. Wave transformation was monitored by 10 wave gauges distributed along the meadow, while velocities were measured at 12 locations as shown in Fig. 3.

3. Wave height attenuation analysis

3.1. Wave height attenuation

The effect of the seagrasses on the wave propagation over the meadow and the resultant energy dissipation can be seen in Fig. 4, where the wave energy spectrum is depicted for three characteristic experimental tests. The spectrum is presented for the resistive wave gauges, WG4, WG6, WG11, WG9 and WG13 at locations $x/L=-0.05$, 0.14, 0.61, 0.89 and 1.17, where x stands for the distance from the meadow front and $L=10.70$ m is the total meadow length. A gradual decrease of the wave energy along the meadow is shown which is due to the drag of the seagrass meadow. Wave energy dissipation is obvious for all components of the wave spectra, especially at peak frequencies. It is also noticed that the wave spectrum located onshore at $x/L=1.17$ shows a larger wave energy than the one located at $x/L=0.89$ inside the meadow. Similar findings are shown in the wave height variation which is depicted in the following figures. Specifically, as the wave exits the submerged vegetation, the wave height slightly increases. The differences between the wave celerity inside and downstream the meadow led to this increase, in similarity with the wave propagation over a submerged porous step (Losada et al., 1997).

The resulting wave height variation over the meadow is shown in Figs. 5 and 6 for various experimental configurations and for stem

Table 1
Wave and *Posidonia oceanica* meadow characteristics.

Water depth at meadow h (m)	Significant wave height H_s (m)	Peak wave period T_p (s)	Wavelength λ (m)	H/λ	h/λ	Meadow density N (stems/m^2)	Meadow submergence ratio $\alpha=h_s/h$
1.70	0.28	2.00	5.92	0.047	0.29	360	0.32
1.70	0.40	3.00	10.69	0.037	0.16	360	0.32
1.70	0.30	4.50	17.34	0.017	0.10	360	0.32
1.50	0.28	2.00	5.78	0.048	0.26	360	0.37
1.50	0.40	3.00	10.21	0.039	0.15	360	0.37
1.50	0.31	4.00	14.37	0.022	0.10	360	0.37
1.30	0.28	2.00	5.60	0.050	0.23	360	0.42
1.30	0.40	3.00	9.67	0.041	0.13	360	0.42
1.30	0.31	4.00	13.50	0.023	0.10	360	0.42
1.10	0.28	2.00	5.36	0.052	0.21	360	0.50
1.10	0.40	3.00	9.04	0.044	0.12	360	0.50
1.10	0.35	3.50	10.81	0.032	0.10	360	0.50
1.10	0.31	4.00	12.53	0.025	0.09	360	0.50
1.70	0.28	2.00	5.92	0.047	0.29	180	0.32
1.70	0.40	3.00	10.69	0.037	0.16	180	0.32
1.70	0.31	4.00	15.17	0.020	0.11	180	0.32
1.50	0.28	2.00	5.78	0.048	0.26	180	0.37
1.50	0.40	3.00	10.21	0.039	0.15	180	0.37
1.50	0.31	4.00	14.37	0.022	0.10	180	0.37
1.30	0.28	2.00	5.60	0.050	0.23	180	0.42
1.30	0.40	3.00	9.67	0.041	0.13	180	0.42
1.30	0.31	4.00	13.50	0.023	0.10	180	0.42
1.10	0.28	2.00	5.36	0.052	0.21	180	0.50
1.10	0.40	3.00	9.04	0.044	0.12	180	0.50
1.10	0.31	4.00	12.53	0.025	0.09	180	0.50

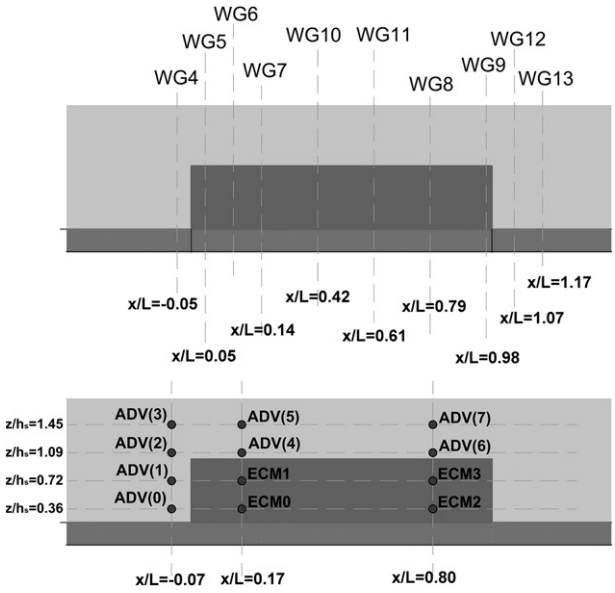

Fig. 3. Location of resistive wave gauges and current-meters along the meadow.

densities of 180 and 360 stems/m^2 respectively. The wave height decay is shown as the ratio of H/H_o, where H is the root-mean-square wave height along the meadow, H_{rms}, and H_o is the root-mean-square wave height before the meadow at WG4, $H_{rms,o}$. It is evident that the wave damping depends strongly on the meadow properties such as the stem density, N and the submergence ratio, α and on the peak wave period, T_p.

This strong relationship between these parameters can be found in the relevant literature, where analytical solutions have been developed in order to describe the wave damping over submerged vegetation. Usually the wave attenuation over seagrasses is described either by an exponential function shown (Eq. (4)) (Kobayashi et al., 1993) or by the expression given in Eq. (5) (Dalrymple et al., 1984; Mendez and Losada, 2004), based on the conservation of energy equation; the energy loss of waves propagating through vegetation is due to the work carried out on the vegetation:

$$K_v = \frac{H}{H_o} = \exp(-k_i x) \tag{4}$$

$$K_v = \frac{H}{H_o} = \frac{1}{1+\beta x} \tag{5}$$

where, K_v is a damping coefficient and k_i and β are parameters related to the plant and wave characteristics and x is the distance along the meadow. Both equations are shown (Dalrymple et al., 1984) to be identical for small values of the arguments k_i and β respectively, which is the case for such wave and seagrass interaction.

Based on the experimental results, an average value of β is obtained for each test and then the theoretical variation for K_v is calculated from Eq. (5) which is also shown in Figs. 5 and 6. The proposed analytical expression fits well the experimental results regarding the wave height exiting the meadow while in the seaward side small differences are observed which are discussed below.

The effect of the submergence ratio on wave attenuation is shown in Fig. 7 where K_v is plotted for the same wave conditions ($H_s = 0.28$ m, $T_p = 2$ s) and meadow density N = 360 stems/m^2 and 180 stems/m^2. For both densities, the incident wave height (measured at $x/L = -0.05$) is reduced by ~15–25%, with a larger attenuation observed for the dense meadow. In the seaward side of the meadow ($x/L = -0.05$) the wave height increases for the dense meadow (360 stems/m^2). This is due to the sudden local decrease of the "water depth", as

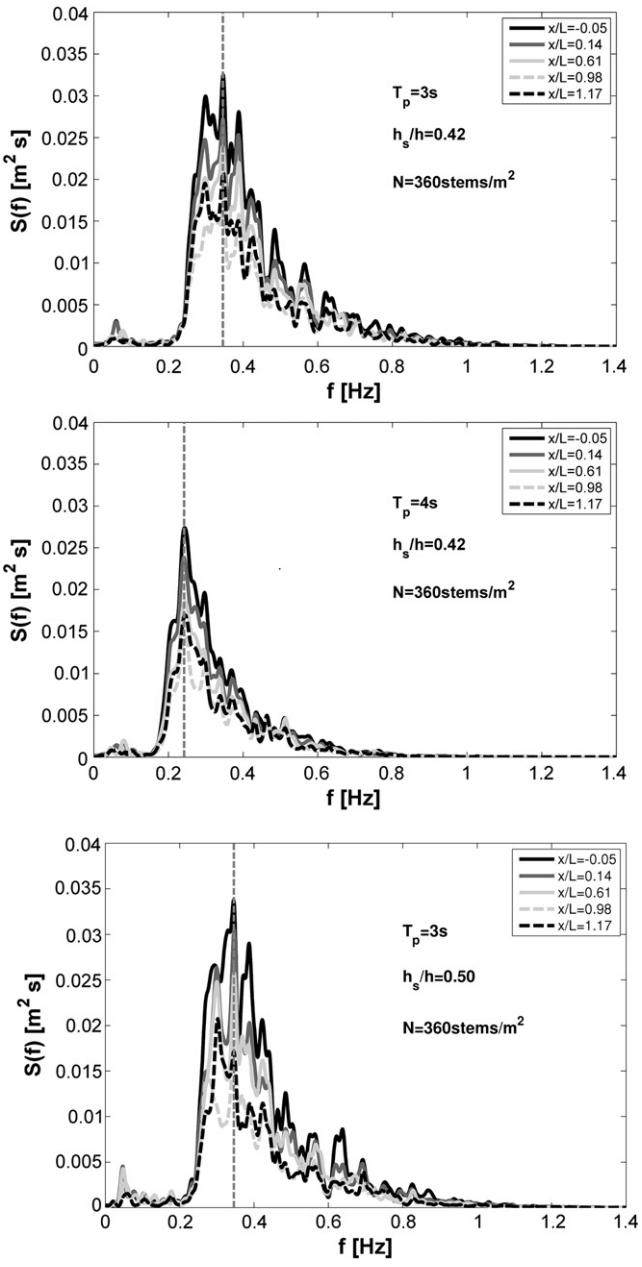

Fig. 4. Wave spectrum transformation along the meadow.

can be seen if the dense meadow is considered as a 'rigid' submerged barrier. This is not the case for the sparse one where the wave height is gradually attenuated. The effect of the submergence ratio on wave attenuation is also evident. The degree of wave attenuation is related to the fraction of the water column occupied by the seagrass as expressed by the submergence ratio and the stem density. This was expected, since the wave energy loss over the meadow is due to the drag force induced by the vegetation, which is higher when a larger fraction of water is within the meadow.

The effect of the dispersion parameter h/λ on wave attenuation is shown in Fig. 8 where K_v is plotted for the same plant configurations (N = 360 stems/m^2 and 180 stems/m^2 respectively, $h_s/h = 0.50$) and variable wave conditions. The longer waves are mostly attenuated with a maximum wave attenuation up to 35% observed for $h/\lambda = 0.09$ and the dense meadow (N = 360 stems/m^2). This can be easily interpreted based on wave kinematics, since for longer waves the highest portion of the water column beneath the free surface is under wave motion, so the plant resistance to the flow is stronger.

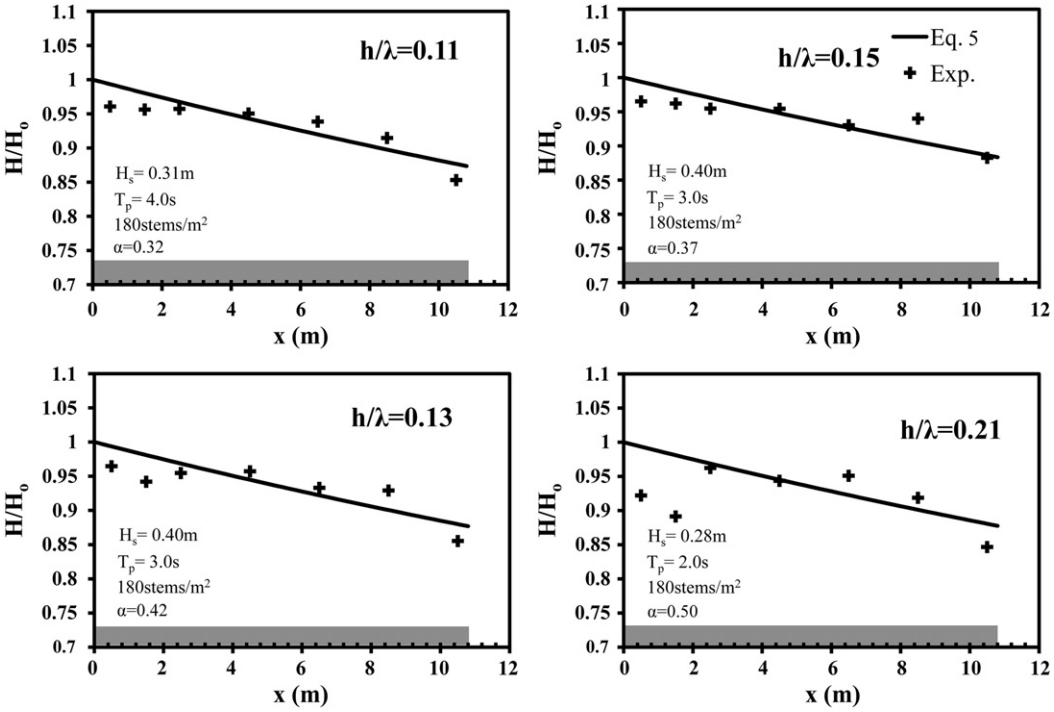

Fig. 5. K_v ($=H/H_o$) variation over the artificial *P. oceanica* meadow length, x, for different experiments ($N=180$ stems/m^2). (+) experimental results, (line) theory as Eq. (5).

The dependence of the β parameter on the above characteristics is shown in Fig. 9, where values of β range from 0.005 to 0.035. For these small values for β, the above mentioned similarity of Eqs. (4) and (5) is verified. It is shown that a 50% increase of the submergence ratio, α (from 0.32 to 0.50), results in an average 117% increase of β. Also a 100% increase of the stem density, N, results in an average 80% increase of β. The effect of the wave period is also significant since a 100% increase of T_p (from 2 s to 4 s) results in an average 115% increase of β.

3.2. Estimation of drag coefficient C_d

To obtain a general expression for estimating the attenuation coefficient K_v which can be considered characteristic for the *P. oceanica*

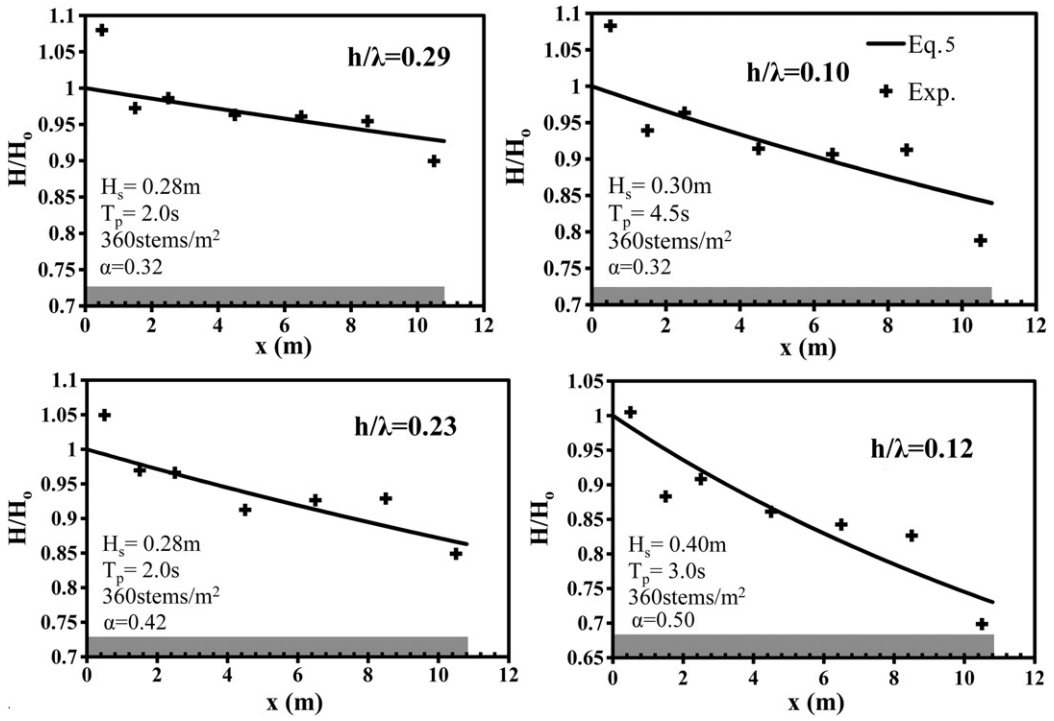

Fig. 6. K_v ($=H/H_o$) variation over the artificial *P. oceanica* meadow length, x, for different experiments ($N=360$ stems/m^2). (+) experimental results, (line) theory as Eq. (5).

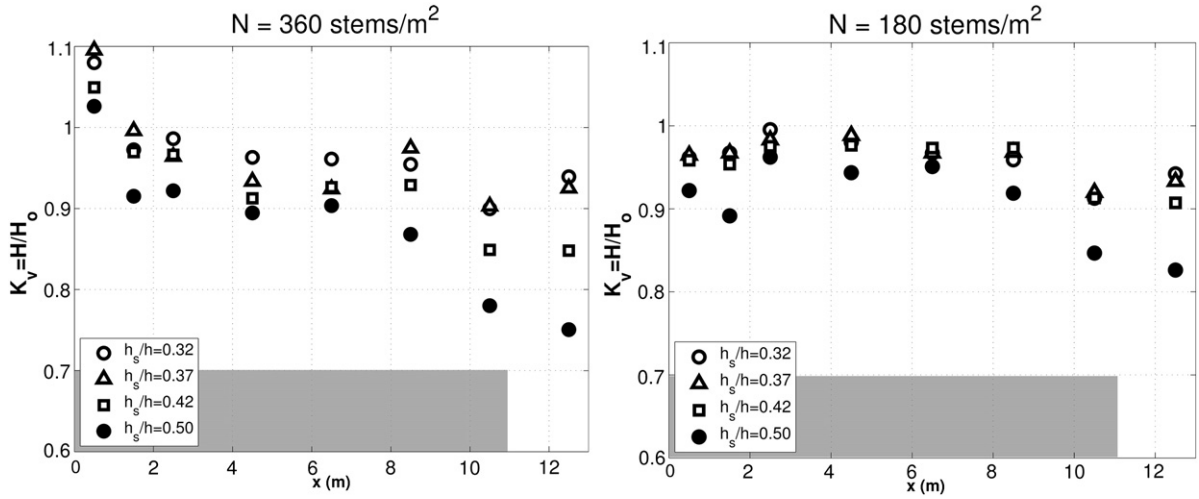

Fig. 7. K_v ($=H/H_o$) variation over the meadow for different submergence ratios h_s/h ($H_s=0.28$ m, $T_p=2$ s).

plant, the analysis of Mendez and Losada (2004) is adopted, which is an extension of the Dalrymple et al. (1984) approach. The same analysis has been conducted also by Bradley and Houser (2009) and Cavallaro et al. (2010) among others. They showed, based on the conservation of wave energy equation that the parameter β used in Eq. (5) for random waves, can be expressed as:

$$\beta = \frac{1}{3\sqrt{\pi}} C_d b_v N H_o k \frac{\sin h^3 k\alpha h + 3\sin hk\alpha h}{(\sin h2kh + 2kh)\sin hkh} \tag{6}$$

where, C_d is the average drag coefficient of the meadow, b_v is the plant area per unit height of each vegetation stand normal to the horizontal velocity (0.01 m for the present experiments) and k is the wave number. In fact C_d is the most important parameter for the calculation of the damping coefficient and is characteristic for each plant related to its biomechanical properties. Based on the results for β, the average C_d can be obtained, by rewriting Eq. (6):

$$C_d = \beta \frac{3\sqrt{\pi}}{b_v N H_o k} \frac{(\sin h2kh + 2kh)\sin hkh}{\sin h^3 k\alpha h + 3\sin hk\alpha h}. \tag{7}$$

For such wave seagrass interaction a relationship between C_d and a characteristic nondimensional flow parameter is desired for the efficient modeling of the hydrodynamic behavior of *P. oceanica* under wave motion. In literature C_d is usually related to the Reynolds number, Re, in the form of Eq. (8):

$$C_d = \alpha + \left(\frac{\beta}{Re}\right)^{\gamma} \tag{8}$$

where the coefficients α, β, γ depend on the plant characteristics (shape of leaves, length and thickness of leaves, density, modulus of elasticity, and stiffness) with values found in literature shown in Table 2. The Reynolds number is given as:

$$Re- = \frac{u_{c,0} \cdot b_v}{\nu} \tag{9}$$

where v is the kinematic fluid viscosity of water (10^{-6} m^2/s) and $u_{c,0}$ is a characteristic velocity, selected as the maximum orbital velocity upward the meadow, at the meadow edge ($z=-h+h_s$) and calculated by applying the linear wave theory, using $H_{rms,0}$ and T_p as the wave height and period corresponding to a monochromatic wave train:

$$u_{c,0} = \frac{\pi H_0}{T} \frac{\cos h(k\alpha h)}{\sin h(kh)}. \tag{10}$$

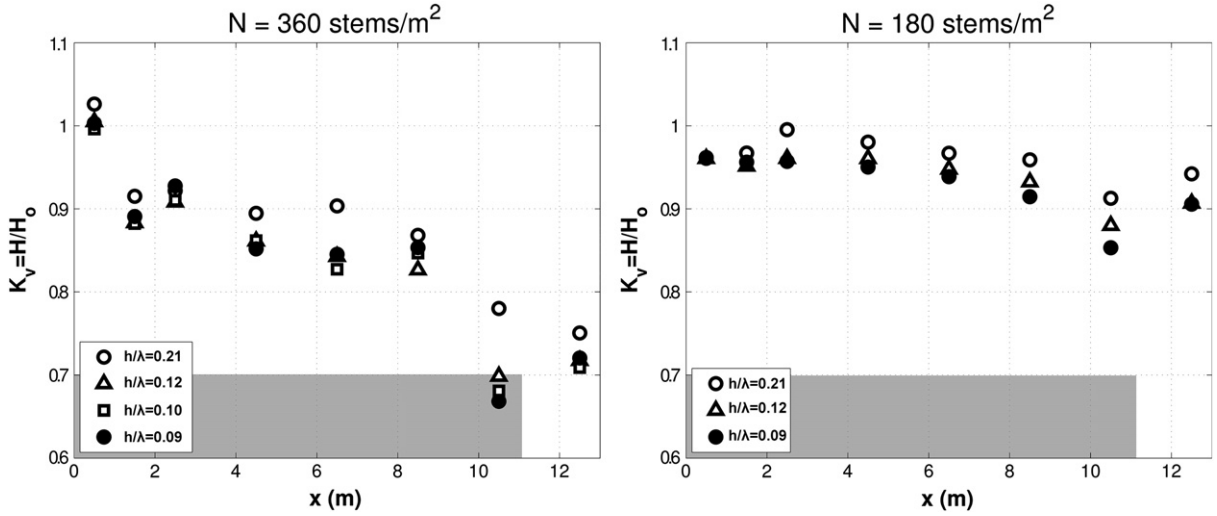

Fig. 8. K_v ($=H/H_o$) variation over the meadow for different h/λ ($h_s/h=0.50$).

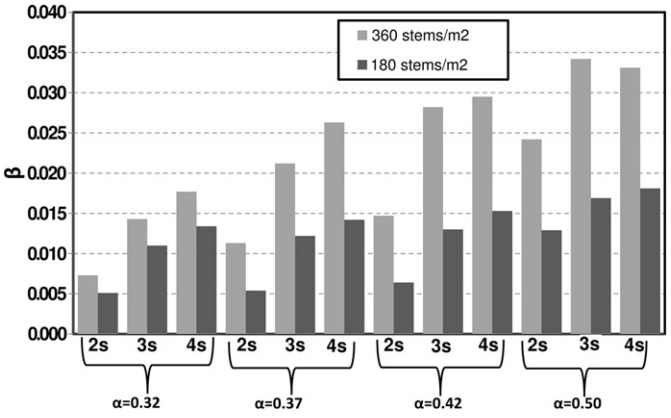

Fig. 9. β parameter variation for various experimental configurations.

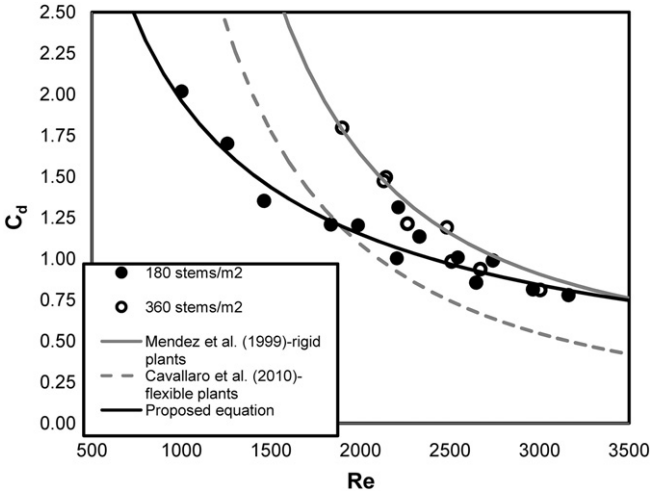

Fig. 10. Variation of C_d with a Reynolds number.

Fig. 10 shows the measured C_d values against the Reynolds number for both stem densities, together with the plot of Eq. (8) for the coefficients α, β and γ taken from the Mendez et al.'s (1999) study on rigid plants and Cavallaro et al. (2010) on flexible *P. oceanica* artificial meadow. The Reynolds number considered in the present study varies from 1000 to 3200, while in the above mentioned studies it varies from 200 to 15,500. Based on the present experimental results for a meadow density of 180 stems/m^2, a new relationship that correlates the drag coefficient and the Reynolds number is proposed for the plant of *P. oceanica* with a correlation coefficient $R^2 = 0.91$:

$$C_d = \left(\frac{2400}{Re}\right)^{0.77}. \quad (11)$$

The results from other experimental studies on wave and submerged vegetation interaction (Augustin et al., 2009) show that such a correlation can be poor. It should be mentioned that for the wave conditions tested, poor correlation was found for the C_d with the Keulegan–Carpenter number K, in the range of $20<K<100$. The proposed C_d formulation is useful in numerical modeling of such wave–sea grass interactions, where the extra terms in the momentum equations, due to the drag force, are expressed in terms of C_d. Also in field applications, the estimation of C_d is simple and based on measurements of the wave conditions of the study area.

The results indicate that the meadow stem's density is important for the evaluation of the proper C_d, as has been shown also in Huang et al. (2011), while the submergence ratio has a minor effect for the tested conditions ($0.32<\alpha<0.50$). It is shown that for the dense meadow (360 stems/m^2) the estimated C_d is greater than the sparse case (180 stems/m^2) and the experimental data for $Re<2500$ tend to follow the curve for the rigid plants proposed by Mendez et al. (1999). Actually for mild wave conditions $Re<2500$ the denser meadows are shown not to be inserted into motion by wave action and the drag force is shown to be the same with the rigid plants' assumption. Moreover it is shown that for $Re>2500$ the results for both densities follow the same trend, showing a possible threshold for indication of dense (to be modeled as porous flow) or sparse vegetation.

It should be mentioned that the wave conditions examined within the present study refer to relatively mild wave conditions ($1000<Re<3200$). Looking closely to the form of Eqs. (8) and (11) and the experimental results as depicted in Fig. 10, the high decrease of the C_d with the increase of Re is shown, for such range of Re. This is not the case for the storm conditions that correspond to Re in the range of 10,000–15,000. For this region C_d has a small decrease with the increase of Re and is asymptotic to a specific value, which is calculated as $C_d \sim 0.20–0.30$ by applying Eq. (11), $C_d \sim 0.40$ for the rigid plants and $C_d<0.10$ for the flexible plants, by applying Eq. (8) with α, β and γ taken from the Mendez et al.'s (1999) and Cavallaro et al.'s (2010) studies respectively. This comparison demonstrates the effect of the stiffness of the plants to the estimated C_d and suggests that the extraction of the outcome of the present study to storm conditions give reasonable results. What is also shown is that the validity of such a relationship in Eq. (8) is subject to the efficient modeling of the mechanical properties of the artificial plant used.

The validity of Eq. (11) can be checked, through the comparison of the measured H_{rms} along the meadow of all the experiments with the predicted H_{rms} based on the use of Eqs. (5), (6) and (11). The results show a satisfactory agreement, with the predicted wave heights being slightly overestimated at all positions along the meadow, except at $x/L = 0.79$, suggesting that such a relationship can be useful for estimating the wave height damping over a *P. oceanica* meadow (Fig. 11).

Table 2
Values of coefficients α, β, γ found in literature.

Study	α	β	γ
Mendez et al. (1999) — rigid plant	0.40	2200	2.2
Cavallaro et al. (2010) — swaying plant	0	2100	1.7
Present study	0	2400	0.77

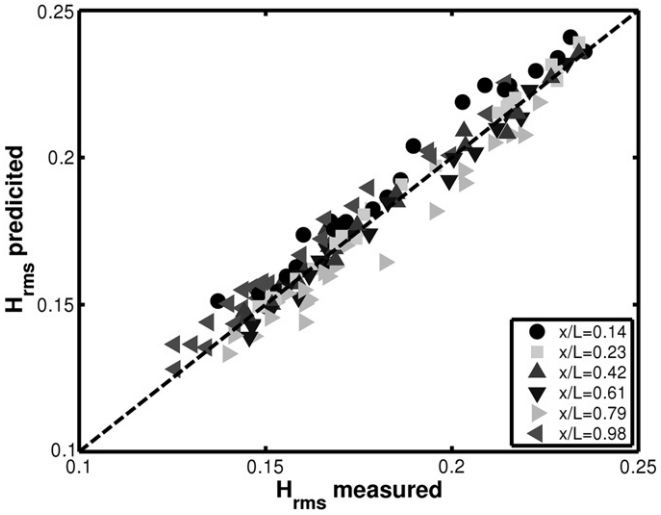

Fig. 11. Comparison between measured and predicted H_{rms}.

4. Wave induced velocities attenuation analysis

In this section, the data of the orbital velocities attenuation by the artificial *P. oceanica* meadow are discussed and a subsequent spectral analysis of the data is performed with the calculation of an attenuation parameter. The purpose of such analysis is to obtain insight on the flow structure above and inside the meadow.

4.1. Wave induced velocity attenuation

The velocities were measured at three vertical locations, upstream the meadow at x/L = −0.07, inside the meadow at x/L = 0.17 and 2 m from the meadow end, at x/L = 0.80. At each vertical location ADVs were installed at four different levels; at 20 cm, 40 cm, 60 cm and 80 cm above the seabed, or at $z/h_s = 0.36$, 0.72, 1.09 and 1.45 respectively, where z denotes the distance from the flume bed and $h_s = 0.55$ m is the seagrass height (Fig. 3). Fig. 12 shows the power spectrum of the horizontal velocity at the four levels. Within the meadow, $z/h_s = 0.36$, the velocities are decreased significantly for all wave components, and the maximum value of the spectrum for the peak period is reduced by 85% when wave exits the meadow (x/L = 0.80). A small shift of the energy from lower to higher frequency components is observed as the wave enters the meadow, from x/L = −0.07 to x/L = 0.17, evident at all four levels. This energy transfer is not clearly shown in the wave height spectrum shown in Fig. 4 for this test. The reduction of velocities is shown also above the meadow at $z/h_s = 1.45$ for the wave exiting the meadow (x/L = 0.80). However for the position just above the top of the seagrass ($z/h_s = 1.09$) the energy at the peak frequencies of the spectrum is amplified even at x/L = 0.80, revealing the effects attributed to the movement of the plant leaves. Regarding the vertical velocities, a gradual decay of the velocities along the meadow is observed at all levels ($z/h_s = 0.36$, 0.72, 1.09 and 1.45) as the wave exits the meadow (Fig. 13). Moreover the vertical velocities are much lower than the horizontal ones for these wave conditions, $h/\lambda = 0.12$.

These findings are shown more clearly in Fig. 14 where the experimental vertical distributions of minimum and maximum horizontal and vertical velocities are shown along the meadow. The velocities are made dimensionless with the maximum free surface velocity at x/L = −0.07 and are plotted together with the velocity profiles derived from the linear wave theory at x/L = −0.07. The velocity attenuation is evident inside the lower canopy position ($z/h_s = 0.36$) as the wave exits the vegetated flume bed (x/L = 0.80), while much above the meadow ($z/h_s = 1.45$) the velocities are slightly attenuated. The complex flow pattern is revealed at the position just above the meadow edge ($z/h_s = 1.09$) where horizontal velocities are increased and vertical velocities are slightly decreased due to the higher interaction between waves and moving leaves. The excess of the positive wave induced horizontal velocities above the meadow ($z/h_s > 1$) and the negative ones below the meadow ($z/h_s < 1$), which is more obvious upstream the meadow (x/L = −0.07), suggests the existence of a local circulation pattern.

In order to analyze the effect of the plant properties on the velocity structure, an analysis based on the power spectrum of the horizontal velocities follows.

4.2. Velocity attenuation parameter

The wave induced velocity spectral densities is calculated for all tests and x/L locations along the meadow. An attenuation parameter (α_j) is calculated to evaluate the changes in the wave-induced spectral flows caused by the canopy and to compare them under different test conditions. It was calculated for the lower canopy at each frequency component of the spectrum, following a method similar to that developed for coral reefs (Lowe et al., 2007):

$$\alpha_j = \left(\varphi_j^2 \frac{S_{U,low}}{S_{U,high}^{IN}}\right)^{0.5} = \left(\varphi_j^2 \frac{S_{U,z=20\ cm}}{S_{U\ z=80\ cm}^{IN}}\right)^{0.5} \quad (12)$$

where $S_{U,low}$ is the wave-induced velocity spectra obtained from the lower ADV ($z_{low} = 0.20$ m) at each of the three x/L locations and $S_U^{IN}{}_{,high}$ is the wave induced flow spectra obtained from the higher ADV ($z_{high} = 0.80$ m) at the location upstream the meadow, at x/L = −0.07. The term φ_j is a correction factor to take into account the predicted vertical increase of the flow magnitude with distance

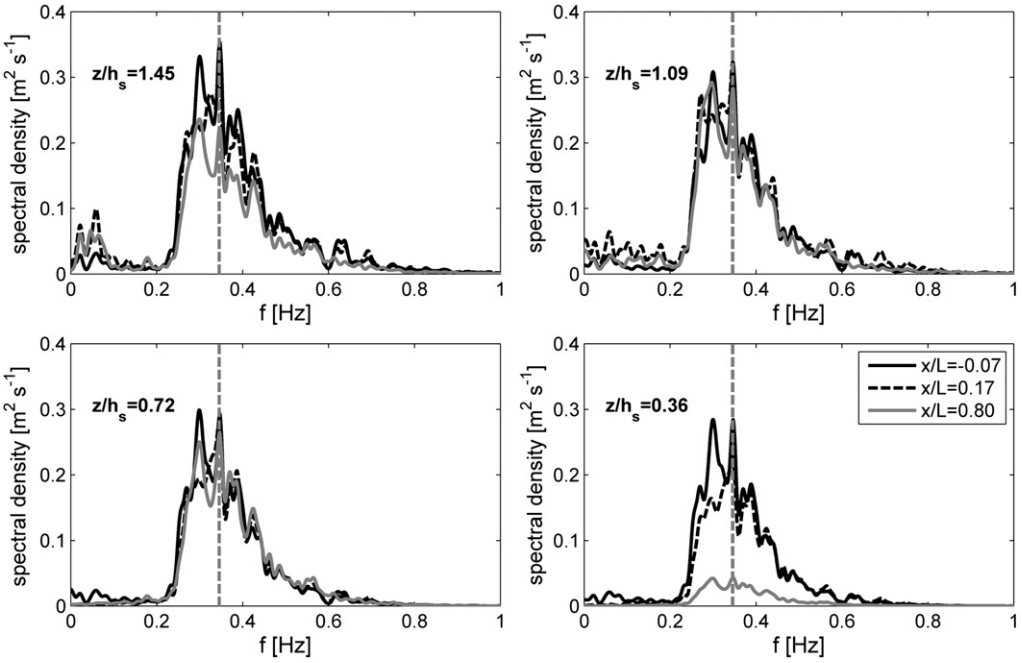

Fig. 12. Power spectrum of measured horizontal velocity for $H_s = 0.4$ m, $T_p = 3$ s, $h/\lambda = 0.12$, $h_s/h = 0.50$ and $N = 360$ stems/m^2.

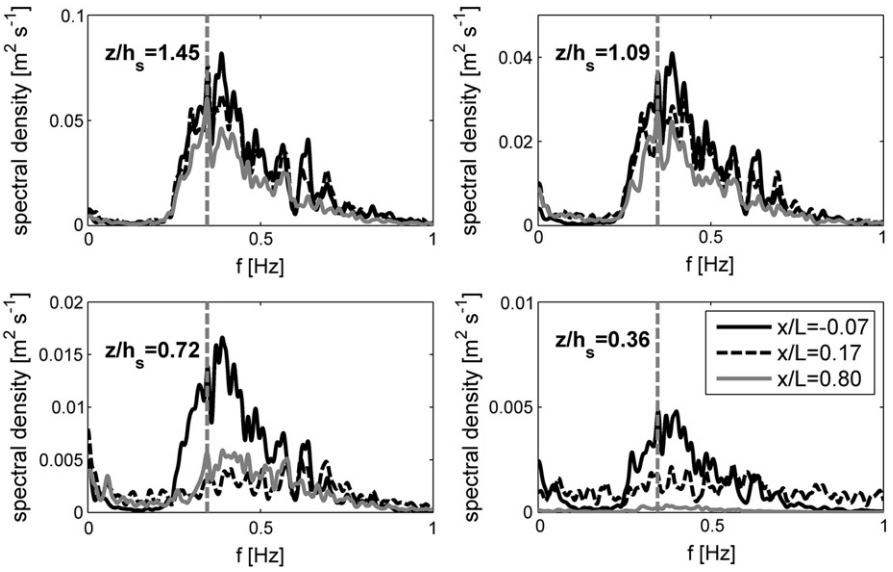

Fig. 13. Power spectrum of measured vertical velocity for $H_s = 0.4$ m, $T_p = 3$ s, $h/\lambda = 0.12$, $h_s/h = 0.50$ and $N = 360$ stems/m^2.

from the flume bed. It is derived from the linear wave theory (Dean and Dalrymple, 1991) and calculated as:

$$\varphi_j = \frac{\cos h\left(k_j z_{high}\right)}{\cos h\left(k_j z_{low}\right)} \tag{13}$$

where z_{high} and z_{low} are the elevations of the highest current-meter ($z_{high} = 0.80$ m) and lowest current-meter ($z_{low} = 0.20$ m). K_j is the wave number evaluated for each component of the spectrum. For each test, the attenuation parameter was calculated at the three x/L locations (x/L = −0.07, 0.17 and 0.80) and for spectral components containing most of the wave energy.

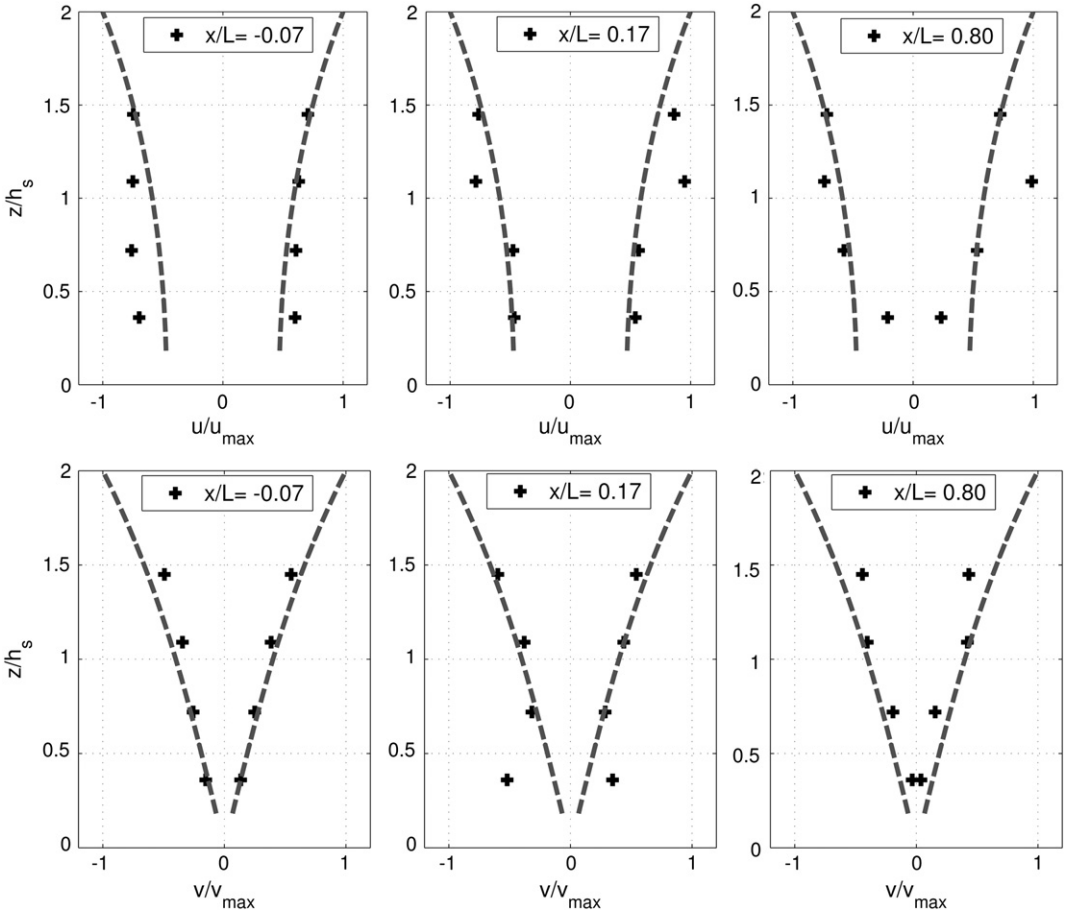

Fig. 14. Vertical distribution of the dimensionless horizontal (above) and vertical (below) velocities for $H_s = 0.4$ m, $T_p = 3$ s, $h/\lambda = 0.12$, $h_s/h = 0.50$ and $N = 360$ stems/m^2. The velocities are made dimensionless with u_{max} and v_{max}, maximum horizontal and vertical free surface velocities ($z/h_s = 2$) from the linear wave theory. (+) experimental results, (line) linear wave theory.

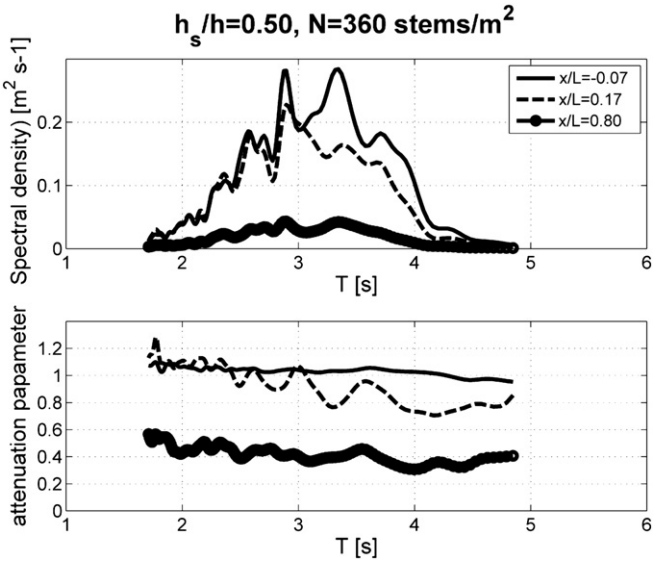

Fig. 15. Spectra of wave induced velocities measured in the lower canopy ($z/h_s = 0.36$) at the three locations along the meadow (above). Attenuation parameter for the spectral components T_j (below).

The spectrum of the of wave induced velocities measured in the lower canopy ($z/h_s = 0.36$) at the three locations along the flume (ADV0, ECM0, ECM2 as in Fig. 3) is shown in Fig. 15, for $H_s = 0.4$ m, $T_p = 3$ s, $h_s/h = 0.50$ and $N = 360$ stems/m^2, together with the attenuation parameter. Upward the meadow ($x/L = -0.07$) the attenuation parameter is about equal to one, showing that the reflection due to the meadow is insignificant. As the wave enters the vegetated bed ($x/L = 0.17$), it is shown that the velocities of the longer wave components ($T_j > T_p = 3$ s) are mostly attenuated, while the short wave components obtain values $\alpha_j > 1$. This reveals a flow field with nonlinear interactions, with a partly energy transfer from the longer to the shorter period wave components. This is more evident from Fig. 16 where the attenuation parameter is depicted as calculated for $H_s = 0.4$ m, $T_p = 3$ s and $N = 360$ stems/m^2, at the three locations along the meadow ($x/L = -0.07$, 0.17 and 0.80). The small values of $\alpha_j \sim 0.4$ at the leeward side of the meadow ($x/L = 0.80$) indicate the efficient velocity reduction for all the submergence ratios at the lower canopy ($z/h_s = 0.36$). The wide reduction on the velocities above the seabed indicates the efficiency of the meadows in minimizing sediment suspension under wave action and eventually erosion.

Minor attenuation in wave energy is observed from the lower submergence ratio, particularly for the shorter period wave components. The influence of the stem density on the attenuation parameter is not

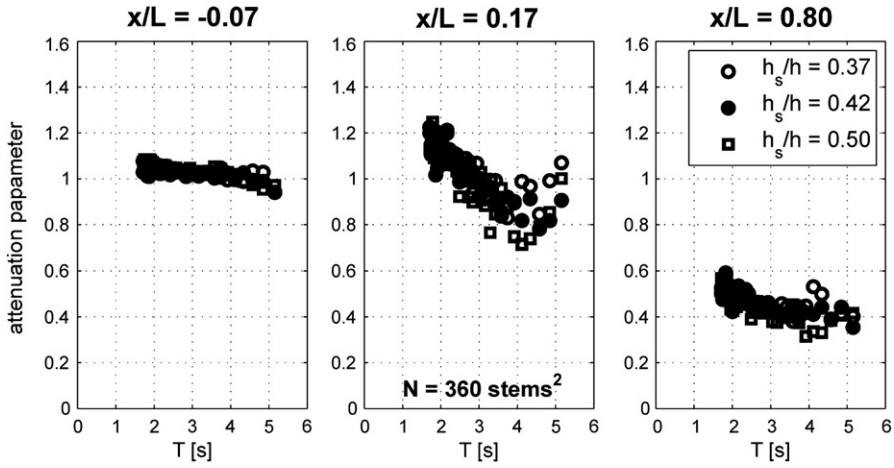

Fig. 16. Attenuation parameter (α_j) calculated for each wave period (T_j) of the wave-induced velocity spectra component. $H_s = 0.4$ m, $T_p = 3$ s, $N = 360$ stems/m^2.

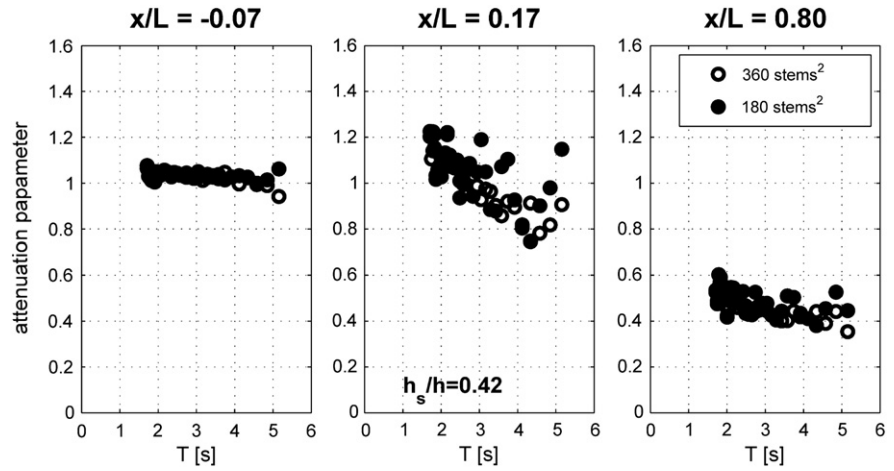

Fig. 17. Attenuation parameter (α_j) calculated for each wave period (T_j) of the wave-induced velocity spectra component. $H_s = 0.4$ m, $T_p = 3$ s, $h_s/h = 0.42$.

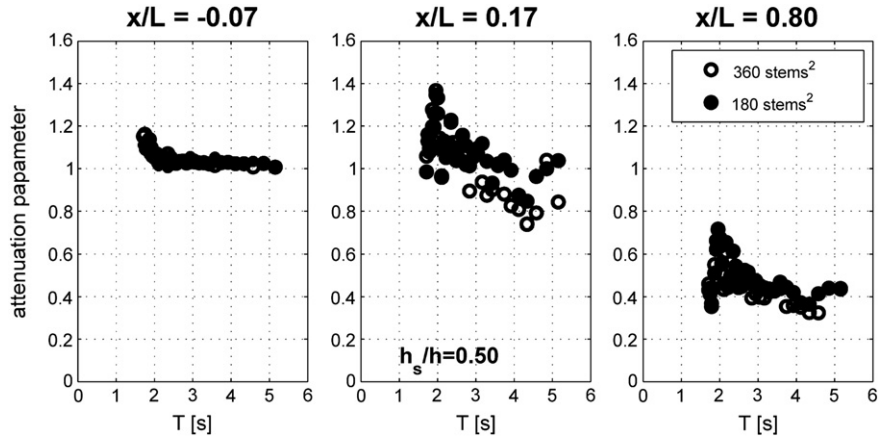

Fig. 18. Attenuation parameter (α_j) calculated for each wave period (T_j) of the wave-induced velocity spectra component. $H_s = 0.4$ m, $T_p = 4$ s, $h_s/h = 0.50$.

significant as the wave exits the meadow ($x/L = 0.80$), as shown from Fig. 17 for the same wave conditions ($H_s = 0.4$ m, $T_p = 3$ s) and submergence ratio ($h_s/h = 0.42$). However at $x/L = 0.17$, the velocities are reduced for the dense meadow ($\alpha_j \sim 0.8$) while for the sparse one they are found unaltered. This is in accordance with the findings from the wave height analysis, where it was shown that the denser meadow acts as a "submerged barrier" as the wave enters the vegetated seabed. Similar results are obtained for the longer wave period test ($H_s = 0.4$ m, $T_p = 4$ s) and for $h_s/h = 0.50$ shown in Fig. 18; longer wave components are mostly attenuated from the canopy, which is in accordance with the findings of the wave height analysis. Similar results were found also in the experimental study of Lowe et al. (2007).

If the velocities measured at the higher located ADVs, at $z = 40$ cm ($z/h_s = 0.72$) and $z = 60$ cm ($z/h_s = 1.09$), are used for the calculation of α_j in Eq. (11), the results for the attenuation parameter are shown in Fig. 19. Regarding the location upstream the meadow ($x/L = -0.07$) the attenuation parameter shows that it is unaffected by the meadow ($\alpha_j \sim 1$) but for the location inside the meadow the variation for the results seems to be affected by the leaves' motion. The attenuation parameter fluctuates arbitrarily between 0.8 and 1.4 at both locations ($x/L = 0.17$ and 0.80), with no specific dependence on the wave period. This reveals that near the meadow edge the motion of the plant leaves highly interacts with the water as indicated by Koch et al. (2006).

5. Conclusions

The main objective of this study was to evaluate the effects of the *P. oceanica* meadow on the wave height formulation and on the wave orbital velocities. Full scale experiments were conducted in the CIEM flume in Barcelona and several wave conditions and plant configurations were tested. The following conclusions can be derived:

1. The wave height distribution follows well the proposed analytical expression found in literature, of the form $1/1+\beta x$, where x is the distance from the meadow boundary and parameter β depends on the plant and wave characteristics. Parameter β is shown to depend strongly on the meadow submergence ratio and stem density and on the wave conditions. Experimental values for β indicate the similarity of this expression to another commonly used, in such wave and vegetation interaction, exponential decay law.
2. For the dense meadow, in its upward side, the wave height slightly increases due to the sudden local decrease of the "water depth". The dense meadow acts as a 'rigid' submerged barrier.
3. The degree of the wave attenuation observed is related to the fraction of the water column occupied by the seagrass as expressed by the submergence ratio and the stem density. The wave damping increases with an increasing submergence ratio and stem density, as expected, since the wave energy loss over the meadow is due

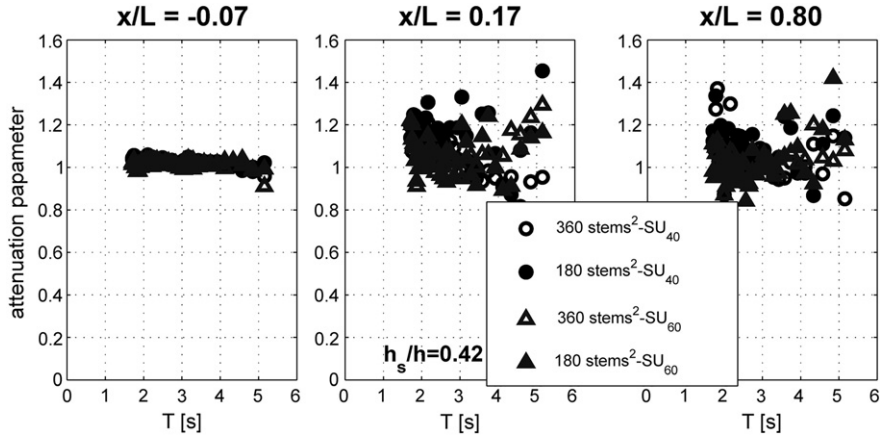

Fig. 19. Attenuation parameter (α_j) for the cases as in Fig. 17 as calculated for the ADVs at $z = 40$ cm and $z = 60$ cm ($SU_{,low} = SU_{,40}$ and $SU_{,low} = SU_{,60}$ respectively).

to the drag force induced by the vegetation, which is higher when a larger fraction of water is within the meadow.

4. The longer waves are mostly attenuated from the meadow with a maximum wave height damping ~35% observed for $h/\lambda = 0.09$ and the dense plant. This was expected since for longer waves, the highest portion of the water column beneath the free surface is under the wave motion, so the plant resistance to the flow is stronger.
5. An empirical relationship for the drag coefficient C_d related to the Reynolds number is obtained. For mild wave conditions, $Re < 2500$, C_d is shown to be the same with the rigid plants' assumption for the dense meadow. The results for the calculated wave heights using the proposed relationship are in satisfactory agreement with that of the measured ones, suggesting that such a relationship can be useful for estimating the wave height damping over a *P. oceanica* meadow.
6. Regarding the velocity structure, it is found that inside the meadow and just above the flume bed, the wave orbital horizontal and vertical velocities are significantly decreased. The velocity attenuation parameter was found to be $\alpha_j \sim 0.4$ for all frequency components of the wave spectrum. This shows explicitly, the ability of the meadows to diminish the sediment suspension under wave action and provide protection against erosion. The velocities at the meadow edge are increased and the wave kinetic energy at the peak frequencies of the spectrum is amplified, while it is reduced mainly at the low frequencies.
7. The longer wave components of the kinetic energy spectrum are mostly attenuated compared to the short wave components, which is in accordance with the findings of the wave height analysis. The partial energy transfer from the longer period to the shorter period wave components, reveals the flow pattern inside the meadow due to the effects introduced in the flow by the plant leaves.

Acknowledgments

The experiments were conducted within the frame of the Hydralab III EU project 022441 (RII3). The authors gratefully acknowledge the assistance of the CIEM laboratory staff.

The support of the European Commission through FP7.2009-1, Contract 244104 — THESEUS ("Innovative Technologies for Safer European Coasts in a Changing Climate"), is also acknowledged.

References

Augustin, L.N., Irish, J.L., Lynett, P., 2009. Laboratory and numerical studies of wave damping by emergent and near emergent wetland vegetation. Coastal Engineering 56, 332–340.

Borum, J., Duarte, C.M., Krause-Jensen, D., Greve, T.M., 2004. European Seagrasses: An Introduction to Monitoring and Management. Monitoring and Managing of European Seagrasses Project.

Bradley, K., Houser, C., 2009. Relative velocity of seagrass blades: implications for wave attenuation in low-energy environments. Journal of Geophysical Research 114, F01004.

Cavallaro, L., Lo Re, C., Paratore, G., Viviano, A., Foti, E., 2010. Response of *Posidonia oceanica* to wave motion in shallow-waters — preliminary experimental results. Proceedings of the International Conference on Coastal Engineering, 1(32) (Shanghai, China).

Chen, S.N., Sanford, L.P., Koch, E.W., Shi, F., North, E.W., 2007. A nearshore model to investigate the effects of seagrass bed geometry on wave attenuation and suspended sediment transport. Estuaries and Coasts 30, 296–310.

Dalrymple, R.A., Kirby, J.T., Hwang, P.A., 1984. Wave diffraction due to areas of energy dissipation. Journal of Waterway, Port, Coastal, and Ocean Engineering 110, 67–79.

Dean, R.G., Dalrymple, R.A., 1991. Water Wave Mechanics for Engineers and Scientists. World Scientific.

den Hartog, C., 1977. Structure, function and classification in seagrass communities. In: McRoy, C.P., Helfferich, C. (Eds.), Seagrass Ecosystems, A Scientific Perspective. Marcel Dekker, New York, Basel, pp. 89–121.

Elginoz, N., Kabdasli, M.S., Tanik, A., 2011. Effects of *Posidonia oceanica* seagrass meadows on storm waves. Journal of Coastal Research SI 64, 373–377.

Folkard, A.M., 2005. Hydrodynamics of model *Posidonia oceanica* patches in shallow water. Limnology and Oceanography 50 (5), 1592–1600.

Fonseca, M.S., Cahalan, J.H., 1992. A preliminary evaluation of wave attenuation by four species of seagrass. Estuarine, Coastal and Shelf Science 35 (6), 565–576.

Ghisalberti, M., Nepf, H.M., 2002. Mixing layers and coherent structures in vegetated aquatic flows. Journal of Geophysical Research 107 (C2), 1–11 (3).

Giraud, G., 1977. Essai de classement des herbiers de *Posidonia oceanica* (L.) Delile. Botanica Marina 487–491.

Granata, T.C., Serra, T., Colomer, J., Casamitjana, X., Duarte, C.M., Gacia, E., 2001. Flow and particle distributions in a nearshore seagrass meadow before and after a storm. Marine Ecology Progress Series 218, 95–106.

Green, E.P., Short, F.T., 2003. World Atlas of Seagrasses. UNEP-WCMC.

Huang, Z., Yao, Y., Sim, S.Y., Yao, Y., 2011. Interaction of solitary waves with emergent, rigid vegetation. Ocean Engineering 38, 1080–1088.

Kobayashi, N., Raichlen, A.W., Asano, T., 1993. Wave attenuation by vegetation. Journal of Waterway, Port, Coastal, and Ocean Engineering 119, 30–48.

Koch, E.W., Sanford, L.P., Chen, S.-N., Shafer, D.J., Smith, J. Mckee, 2006. Waves in seagrass systems: review and technical recommendations. Technical Report, ERDC TR-06-15. US Army Corps of Engineers®.

Li, C.W., Yan, K., 2007. Numerical investigation of wave–current–vegetation interaction. Journal of Hydraulic Engineering 133 (7), 794–803.

Li, C.W., Zhang, M.L., 2010. 3D modelling of hydrodynamics and mixing in a vegetation field under waves. Computers & Fluids 39 (4), 604–614.

Losada, I.J., Patterson, M.D., Losada, M.A., 1997. Harmonic generation past a submerged porous step. Coastal Engineering 31, 281–304.

Lowe, R.J., Falter, J.L., Koseff, J.R., Monismith, S.G., Atkinson, M.J., 2007. Spectral wave flow attenuation within submerged canopies: implications for wave energy dissipation. Journal of Geophysical Research 112, C05018.

Lowe, R.J., Shavit, U., Falter, J.L., Koseff, J.R., Monismith, S.G., 2008. Modeling flow in coral communities with and without waves: a synthesis of porous media and canopy flow approaches. Limnology and Oceanography 53 (6), 2668–2680.

Luhar, M., Coutu, S., Infantes, E., Fox, S., Nepf, H., 2010. Wave-induced velocities inside a model seagrass bed. Journal of Geophysical Research 115, C12005.

Manca, E., Stratigaki, V., Prinos, P., 2010. Large scale experiments on spectral wave propagation over *Posidonia oceanica* seagrass. Proceedings of the 6th International Symposium on Environmental Hydraulics, Athens, Greece, vol. 1, pp. 463–468.

Mendez, F.J., Losada, I.J., 2004. An empirical model to estimate the propagation of random breaking and nonbreaking waves over vegetation fields. Coastal Engineering 51, 103–118.

Mendez, F.J., Losada, I.J., Losada, M.A., 1999. Hydrodynamics induced by wind waves in a vegetation field. Journal of Geophysical Research 104 (C8), 18383–18396.

Nikklas, K., 1992. Plant Biomechanics: An Engineering Approach to Plant Form and Function. Univ. Chicago Press, Chicago.

Ota, T., Kobayashi, N., Kirby, J.T., 2004. Wave and current interactions with vegetation. Proceedings of 29th International Coastal Engineering Conference, World Scientific, Singapore, pp. 508–520.

de Oude, R., Augustijn, D.C.M., Wijnberg, K.M., Dekker, F., de Vries, M.B., Suzuki, T., 2010. Bioengineering in front of a River dike: wave attenuation by vegetation. Proceedings of the 6th International Symposium on Environmental Hydraulics, Athens, Greece, vol. 1, pp. 253–258.

Sánchez-González, J.F., Sánchez-Rojas, V., Memos, C.D., 2011. Wave attenuation due to *Posidonia oceanica* meadows. Journal of Hydraulic Research 49, 503–514.

Stratigaki, V., Manca, E., Prinos, P., Losada, I.J., Lara, J.L., Sclavo, M., Amos, C.L., Cáceres, I., Sánchez-Arcilla, A., 2011. Large-scale experiments on wave propagation over *Posidonia oceanica*. Journal of Hydraulic Research 49 (Suppl.1), 31–43.

Suzuki, T., Dijkstra, J., 2007. Wave propagation over strongly varying topography: cliffs and vegetation. Proceedings of 32nd IAHR Congress, Venice, Italy (CD-ROM).

Tigny, V., Ozer, A., De Falco, A.G., Baroli, M., Djenidi, S., 2007. Relationship between the evolution of the shoreline and the *Posidonia oceanica* meadow limit in a Sardinian coastal zone. Journal of Coastal Research 23, 787–793.

Verduin, J.J., Backhaus, J.O., 2000. Dynamics of plant–flow interactions for the seagrass *Amphibolis antarctica*: field observations and model simulations. Estuarine, Coastal and Shelf Science 50, 185–204.